

1 **TITLE:** Temperature effects on individual-level parasitism translate into predictable effects on  
2 parasitism in populations

3

4

5

6

## ABSTRACT

7 Parasitism is expected to change in a warmer future, but the direction and magnitude of this  
8 change is uncertain. One challenge is understanding whether warming effects will be similar on  
9 parasitism within or on individual hosts (e.g., parasite load) compared to on population-level  
10 parasitism (e.g., prevalence,  $R_0$ ). We adapted a simple temperature-dependent model and  
11 simulated several scenarios for individual- and population-level parasitism. Our model found that  
12 small differences in the underlying biology of host–parasite systems can substantially alter the  
13 expected relationship between the thermal optima of parasitism across levels of organization. In  
14 thirteen empirical host–parasite systems, we found a strong positive correlation between the  
15 thermal optima of individual- and population-level parasitism, suggesting that the effects of  
16 warming on parasitism may often be in the same direction across levels. We also found that  
17 parasitism thermal optima were close to host performance thermal optima in mosquito–parasite  
18 systems but not in non-mosquito–parasite systems. Generally, our results suggest that  
19 information on the temperature-dependence, and specifically the thermal optima, of a host–  
20 parasite system at either the individual- or population-level should provide a useful—though not  
21 quantitatively exact—baseline for predicting temperature-dependence at the other level in a  
22 variety of host–parasite systems.

23

24

25

## 26 INTRODUCTION

27 Climate change is causing organisms to increasingly face temperatures warmer than their  
28 optima for physiological performance. These changes in temperature can alter species  
29 interactions (Thomas & Blanford 2003; Kordas *et al.* 2011), and there is now growing evidence  
30 that climate change has impacted interactions between individual hosts and their parasites as well  
31 as parasite dynamics and outbreaks in host populations (Koelle *et al.* 2005; Bruno *et al.* 2007;  
32 Rohr *et al.* 2011; Ben-Horin *et al.* 2013; Lafferty & Mordecai 2016; Harvell *et al.* 2019; Claar &  
33 Wood 2020). Predicting the effects of temperature and changing climate on infectious disease is  
34 an urgent priority (Altizer *et al.* 2013), yet research tends to focus on the level of either an  
35 individual host's biology or of host populations, but rarely both.

36 Understanding how individual-level *per capita* interactions in host–parasite systems scale  
37 to the population level is key for mitigating disease (Fenton 2008). Indeed, the many biological  
38 processes that occur in host–parasite systems occur across more than one level of biological  
39 organization, and bridging these levels is an important research area (Handel & Rohani 2015).  
40 These processes include those that affect individual host performance, individual parasite  
41 performance, host population dynamics, parasite population dynamics within a host, and parasite  
42 population dynamics among hosts within a population. Crucially, each of these processes and the  
43 traits that underlie them may be temperature dependent. However, whether we should expect the  
44 effects of temperature on individual-level parasitism (e.g., on parasite load or on within-host  
45 parasite population growth rate) to match the effects of temperature on population-level  
46 parasitism (e.g., on parasite prevalence or on the basic reproduction number  $R_0$ ) remains an open  
47 research gap, as does whether small differences in the underlying host–parasite interaction or  
48 thermal biology should affect how thermal effects scale between levels. Understanding the

49 effects of temperature on both individuals and populations is critical for disease mitigation  
50 efforts as the world warms because if the effects are similar across levels of organization, we can  
51 leverage observations of the thermal dependence of parasitism at one level to inform predictions  
52 in more complex systems. However, if effects differ across levels, using observations on the  
53 thermal dependence at one level to extrapolate to the other could provide erroneous predictions  
54 for how warming will affect disease in a system.

55         Obtaining, summarizing, and comparing entire thermal responses can be difficult and  
56 sometimes unfeasible. Fortunately, most thermal response curves have a characteristic non-linear  
57 shape with a single thermal optimum at which performance is maximized ( $T_{opt}$ ) (Huey &  
58 Stevenson 1979; Huey & Kingsolver 1989; Angilletta 2006). In this study, we therefore focus on  
59 and compare thermal optima, as this data is more widely available for many host–parasite  
60 systems than full thermal response curves. Though it does not represent the complete thermal  
61 response,  $T_{opt}$  is a useful metric for comparison both across levels of organization and among  
62 taxa because it determines the range of temperatures at which warming has a positive effect on  
63 parasitism (for  $T < T_{opt}$ ) versus a negative effect (for  $T > T_{opt}$ ). Other metrics, such as thermal  
64 breadth and the critical thermal minimum and maximum, would provide additional information  
65 about how climate change could affect host–parasite interactions at the margins of thermal  
66 tolerance.

67         The thermal optima of parasitism could either match or differ across biological levels of  
68 organization. First, we may expect the optimal temperature for parasitism at the individual level  
69 to reflect the optimal temperature of parasitism in populations because processes across the two  
70 levels can be linked (Ewald 1983; Frank 1996; Mideo *et al.* 2011; Handel & Rohani 2015). For  
71 example, if the rate-limiting or rate-determining process for population-level parasitism is

72 directly related to individual-level parasitism, the effects of temperature on individual-level  
73 parasitism may propagate directly to the population level. From this perspective, the thermal  
74 optima of parasitism at the two levels are unlikely to be independent in many systems. This  
75 could occur if the number of parasites within a host (i.e., individual-level parasitism) is the rate-  
76 determining process affecting the rate of parasite transmission (Ben-Ami *et al.* 2008; McCallum  
77 *et al.* 2017) or the rate at which hosts are killed by the parasite (Day 2001), both of which  
78 subsequently affect population-level parasitism metrics such as  $R_0$  or prevalence (Anderson &  
79 May 1979).

80         On the other hand, temperature may not have the same effects across levels even in cases  
81 where population-level parasitism is dependent on the dynamics of individual-level parasitism.  
82 Indeed, when considering the effects of anti-parasite treatments instead of temperature, models  
83 and field experiments have shown that the effects of treatments on individual hosts do not  
84 necessarily lead to equivalent effects in host populations (Fenton 2013; Pedersen & Antonovics  
85 2013). The process of parasite transmission among hosts can potentially decouple population  
86 dynamics of hosts and parasites from dynamics within host individuals, particularly if the traits  
87 that shape the transmission process are temperature dependent. For example, individual activity  
88 rate can vary with temperature (Casey 1976), thereby modifying the contact rate between  
89 susceptible and infected individuals and the overall transmission rate. If the thermal optima of  
90 traits that affect transmission are much warmer or much cooler than that of individual-level  
91 parasitism, we may expect the thermal optimum of population-level parasitism to be pulled away  
92 from the individual-level optimum towards that of these traits.

93         Beyond exploring correlations between the thermal optima of parasitism across levels,  
94 considering how the optima for parasitism are related to the optima for their uninfected potential

95 hosts can provide a more holistic view of how warming should affect a host–parasite system.  
96 One potential framework for doing this is the thermal mismatch hypothesis (Cohen *et al.* 2017).  
97 This hypothesis predicts that parasitism is maximized at temperatures away from the host’s  
98 optimum—i.e., at cool temperatures for warm-adapted species and at warm temperatures for  
99 cold-adapted species—at both the host individual and host population levels (i.e., individual- and  
100 population-level parasitism thermal responses should peak at temperatures offset from the host  
101 optimum in what is called a thermal mismatch)(Cohen *et al.* 2017, 2019a, b). Thermal  
102 mismatches were first documented in amphibian–chytrid fungus (*Batrachochytrium*  
103 *dendrobatidis*, *Bd*) systems at both the individual and population levels (Cohen *et al.* 2017).  
104 More recently, Cohen et al. (2020) analyzed >2000 host–parasite combinations at the population  
105 level and found evidence for population-level thermal mismatches: hosts from cool climates had  
106 increased disease prevalence at warm temperatures and vice versa. However, outside of  
107 amphibian–*Bd* systems, it is unclear if systems with thermal mismatches at the population level  
108 will also exhibit thermal mismatches at the individual level. How the optimal temperatures for  
109 individual- and population-level parasitism compare to the optimal temperature for the host may  
110 mediate how climate change will affect host–parasite interactions: decreased host performance at  
111 warmer temperatures could either be compounded by increasing parasitism or mitigated by  
112 decreased parasitism.

113         Here, we first develop simple temperature-dependent models for individual-level  
114 parasitism and population-level parasitism to examine the temperature dependence of parasitism  
115 across levels. We then simulate several different scenarios—in which thermal responses of  
116 population-level processes are or are not related to the thermal responses of individual-level  
117 parasitism—to investigate how changes in the underlying processes and thermal biology of a

118 host–parasite system can alter the expected relationship between parasitism  $T_{opt}$  across levels.  
119 Next, after using our model to explore possible relationships between parasitism  $T_{opt}$  across  
120 levels, we sought to describe the observed relationship in nature. We identify thirteen systems  
121 that match our data requirements and re-analyze the data to investigate if the thermal optimum of  
122 population-level parasitism is positively related to the thermal optimum of individual-level  
123 parasitism across empirical host–parasite systems. Finally, we compare thermal optima of  
124 individual- and population-level parasitism to the thermal optimum of host performance in the  
125 thirteen systems to test if the thermal mismatch hypothesis holds across levels in these systems.  
126 Our findings provide a first step towards finding general rules for how warming temperatures  
127 will affect parasitism across biological levels of organization.

128  
129  
130  
131

## METHODS

132

### *Model*

133 To formalize our intuitive arguments for why we may or may not expect the thermal  
134 optimum of parasitism in individual hosts to occur at the same temperature as the thermal  
135 optimum for parasitism in host populations, we adapted a simple temperature-dependent model  
136 for disease spread in a population that can be related to the thermal response for parasitism in an  
137 individual host. Here, we define host individual-level parasitism as parasite load, or the number  
138 of parasites within or on the host.

139 We first described the thermal response of individual-level parasitism using a Brière  
140 function. The Brière function (Eq. 1) is an asymmetrical unimodal function that is often used to  
141 describe thermal performance in biological systems (Briere *et al.* 1999), where  $c$  is a positive rate

142 constant,  $T_{min}$  and  $T_{max}$  are the minimum and maximum temperatures, respectively,  $T$  is  
143 temperature, and  $B(T)$  is set to 0 when  $T > T_{max}$  or  $T < T_{min}$ .

$$144 \quad B(T) = cT(T - T_{min})(T_{max} - T)^{1/2} \quad \text{Eq. 1}$$

145 Next, we developed a simple trait-based model of population-level parasitism by  
146 modeling the basic reproduction number of the parasite ( $R_0$ ; Eq. 2):

$$147 \quad R_0 = \frac{\chi(T) \cdot \sigma(T) \cdot S(T)}{\mu(T) + \alpha(T) + \gamma(T)} \quad \text{Eq. 2}$$

148 Here,  $\chi$  is the contact rate between susceptible and infected hosts,  $\sigma$  is the probability of  
149 infection after contact,  $S$  is the density of susceptible hosts,  $\mu$  is the background mortality rate,  $\alpha$   
150 is the parasite-induced mortality rate, and  $\gamma$  is the host recovery rate. We modeled all six  
151 parameters as temperature-dependent, and for all parameters except  $\mu(T)$  we assumed thermal  
152 responses described by the Brière function (the same functional form used to describe the  
153 thermal response of individual-level parasitism; Eq. 1). We modeled the thermal response of  
154 background mortality rate using a concave-up quadratic function where mortality is minimized at  
155 the thermal optimum and increases at cooler and warmer temperatures, as mortality often shows  
156 relatively symmetrical responses across temperature (van der Have 2002; Angilletta 2009).

157 We simulated the model by randomly drawing different thermal response function  
158 parameters  $\{c, T_{min}, T_{max}\}$  for each temperature-dependent trait (individual-level parasitism and  
159 parameters in Eq. 2). For each of 1000 simulations,  $T_{min}$  was drawn from a uniform distribution  
160 between 0-15,  $T_{max}$  was equal to  $T_{min}$  plus a value drawn from a uniform distribution between 10-  
161 20, and the rate constant  $c$  was drawn from a uniform distribution between 0.5-1.3. Similarly, for  
162 the concave-up quadratic function that describes background mortality rate, in each of the 1000  
163 simulations we drew parameter  $a$  from a uniform distribution between 0.0008-0.0009,  $b$  from a  
164 uniform distribution between 0.02-0.03, and  $c$  from a uniform distribution between 0.1-1.

165 Thermal responses were scaled to realistic magnitudes for each temperature-dependent trait (e.g.,  
166 all thermal responses for the contact rate parameter were scaled by a factor of 0.001), and we set  
167 background mortality rate to a minimum of 0.005 (see Supporting Information for more detail).

168 To explore if changes in the underlying biology of the host–parasite systems can alter the  
169 expected relationship between parasitism  $T_{opt}$  across levels, we modeled four main scenarios: (1)  
170 all temperature-dependent traits were independent; (2) parasite-induced mortality rate was  
171 proportional to parasite load (Anderson & May 1978); (3) per-contact infection probability was  
172 proportional to parasite load (McCallum *et al.* 2017); and (4) both parasite-induced mortality and  
173 per-contact infection probability were proportional to parasite load. We also explored seven  
174 additional model scenarios to determine the sensitivity of our results to our assumptions  
175 regarding both thermal response shape and the structure of the mechanistic model for population  
176 disease spread. These scenarios included changes to how thermal response function parameters  
177 were drawn, the breadth of the thermal response functions, the minimum parasite load across the  
178 temperature range, and the model used to describe population-level disease spread (see  
179 Supporting Information for more details). While the model scenarios explored in the main text  
180 and the Supporting Information represent only a small subset of the possible relationships  
181 between the thermal dependence of parasitism across levels, our aim was to investigate whether  
182 small changes to the underlying biology can result in qualitatively different patterns in the  
183 relationship of thermal optima in parasitism across levels, rather than to exhaustively explore  
184 potential outcomes.

185

186

187



188 *Empirical systems*

189 After using our model to investigate potential relationships for the thermal optima of  
190 parasitism across levels, we sought to describe the observed relationship in empirical systems.  
191 We searched for systems for which measures of host performance (e.g., lifetime reproduction),  
192 individual-level parasitism (e.g., parasite load, parasite reproduction within the host, time spent  
193 infected), and population-level parasitism (e.g.,  $R_0$ , prevalence) were documented across  
194 temperatures, allowing us to identify  $T_{opt}$  for each of the measures. While not an exhaustive list,  
195 we identified thirteen systems that matched these requirements (Table 1): four mosquito–virus  
196 systems (Mordecai *et al.* 2013; Shocket *et al.* 2018a; Tesla *et al.* 2018; Mordecai *et al.* 2019;  
197 Shocket *et al.* 2020), four mosquito–malaria parasite systems (Villena *et al.* 2020), two  
198 *Daphnia*–parasite systems (*D. magna*–*O. colligata*, Kirk *et al.* 2018, 2020; *D. dentifera*–*M.*  
199 *bicuspidata*, Shocket *et al.* 2018b), two amphibian–*B. dendrobatidis* (*Bd*, the causative agent of  
200 chytridiomycosis) systems (Cohen *et al.* 2017), and one crab–rhizocephalan barnacle parasite  
201 system (*E. depressus*–*L. Panopaei*, Gehman *et al.* 2018). While the mosquito systems are mainly  
202 studied with respect to human disease, here we leverage the rich data on their thermal  
203 dependence to explore thermal scaling of the mosquito–parasite interaction, which in turn affects  
204 transmission to humans.

205 Host performance, individual-level parasitism, and population-level parasitism were  
206 measured using different metrics in different systems (Table 1; Supporting Information). We  
207 report a single host  $T_{opt}$  value for eleven of the systems, but two host  $T_{opt}$  values (individual and  
208 population) for the amphibian systems. This is because individual-level parasitism for cold-  
209 adapted and warm-adapted amphibians was measured in the lab across one and two host species,  
210 respectively (Cohen *et al.* 2017), but the thermal response of population-level parasitism was

211 reported as *Bd* prevalence in the field as a function of environmental temperature for 235  
212 surveyed species, where cold- and warm-adapted amphibians were categorized as those at  
213 locations where 50-year mean temperature was  $<15^{\circ}\text{C}$  or  $>20^{\circ}\text{C}$ , respectively (Cohen *et al.*  
214 2017). We therefore used separate  $T_{\text{opt}}$  values for our individual-level host performance  
215 (measured as thermal preference in the lab) and population-level host performance (measured as  
216 the mean climatic temperature experienced in the field across surveyed species).

217 While we were generally constrained to use whichever metric of parasitism or host  
218 performance was reported for a study, we had access to thermal response data for several  
219 different metrics in the mosquito–parasite systems. We chose to use infected days as our measure  
220 of individual-level parasitism in these eight systems because it is a composite metric using  
221 thermal performance data on parasite development rate within the mosquito, vector competence  
222 (the mosquito’s ability to acquire and transmit the parasite), and mosquito survival. We were also  
223 interested in how this choice affected our findings of how closely  $T_{\text{opt}}$  of individual-level  
224 parasitism matched  $T_{\text{opt}}$  of population-level parasitism and  $T_{\text{opt}}$  of host performance. Generally,  
225 using vector competence as a metric of individual-level parasitism gave similar results to our  
226 main metric of infected days, but parasite development rate tended to exhibit higher  $T_{\text{opt}}$  values  
227 than the other two metrics (Fig. S10). The Supporting Information contains further details on  
228 both our model and the methods used to analyze the empirical systems.

229 Using these thirteen systems, we tested for a significant correlation by comparing  
230 population-level parasitism  $T_{\text{opt}}$  to individual-level parasitism  $T_{\text{opt}}$  using the *cor.test* function in  
231 the R package *stats* (R Core Team 2020; method = *pearson*). In some of these systems, metrics  
232 used to calculate individual-level parasitism  $T_{\text{opt}}$  are also a subset of the metrics used to calculate  
233 population-level parasitism  $T_{\text{opt}}$ . For example, the thermal response of mosquito mortality rate is

234 one of several components used to calculate individual-level parasitism in mosquito–parasite  
235 systems, and also one of many components used to calculate population-level parasitism in the  
236 same systems. As a result, observed thermal optima for population-level parasitism are not  
237 independent from observed thermal optima for individual-level parasitism. While this can affect  
238 the interpretation of the observed correlation across systems and whether or not it should be  
239 considered statistically significant, we argue that the partial dependence of population-level  
240 parasitism on what occurs at the individual-level is biologically realistic for many systems.  
241 Finally, using the same systems, we compared  $T_{\text{opt}}$  for individual- and population-level  
242 parasitism to  $T_{\text{opt}}$  of host performance to determine if parasitism generally peaked at  
243 temperatures away from host thermal optima as predicted by the thermal mismatch hypothesis  
244 (Cohen *et al.* 2017, 2019a, b), and if so, whether these thermal mismatches at the individual level  
245 corresponded with thermal mismatches at the population level.

246  
247

248 TABLE 1. Thermal optima of parasitism and host performance for thirteen host – parasite  
 249 systems.  
 250

Host – parasite system	Measure of host performance	Measure of individual-level parasitism	Measure of population-level parasitism	Host performance $T_{opt}$ (°C)	Individual-level parasitism $T_{opt}$ (°C)	Population-level parasitism $T_{opt}$ (°C)	Reference
<i>Culex pipiens</i> – West Nile virus	Adult reproduction weighted by lifespan	Infected days	$R_0$	15.9	23.5	24.5	Shocket et al. 2020
<i>Aedes aegypti</i> - dengue virus	Adult reproduction weighted by lifespan	Infected days	$R_0$	27.6	29.3	29.1	Mordecai et al. 2017
<i>Aedes aegypti</i> - Zika virus	Adult reproduction weighted by lifespan	Infected days	$R_0$	27.7	28.9	28.9	Tesla et al. 2018
<i>Culex annulirostris</i> – Ross River virus	Adult reproduction weighted by lifespan	Infected days	$R_0$	25.6	24.0	26.4	Shocket et al. 2018a
<i>Anopheles gambiae</i> - <i>Plasmodium vivax</i>	Adult reproduction weighted by lifespan	Infected days	Transmission suitability	24.4	23.6	25.0	Villena et al. 2020
<i>Anopheles gambiae</i> - <i>Plasmodium falciparum</i>	Adult reproduction weighted by lifespan	Infected days	Transmission suitability	24.4	23.4	25.0	Villena et al. 2020
<i>Anopheles stephensi</i> - <i>Plasmodium vivax</i>	Adult reproduction weighted by lifespan	Infected days	Transmission suitability	24.0	23.0	24.6	Villena et al. 2020
<i>Anopheles stephensi</i> - <i>Plasmodium falciparum</i>	Adult reproduction weighted by lifespan	Infected days	Transmission suitability	24.0	22.9	24.8	Villena et al. 2020
Cold-adapted amphibians - <i>Batrachochytrium dendrobatidis</i>	Temperature preference for individuals; mean climatic temperature for populations †	Parasite growth rate on host	Prevalence	17.9 (10.5) †	26.0	20.5	Cohen et al. 2017
Warm-adapted amphibians - <i>Batrachochytrium dendrobatidis</i>	Temperature preference for individuals; mean climatic temperature for populations †	Parasite growth rate on host	Prevalence	23.5 (23.9) †	12.0	15.9	Cohen et al. 2017
<i>Eurypanopeus depressus</i> - <i>Loxothylacus panopaei</i>	Uninfected host survival	Parasite lifetime reproduction	$R_0$	18.3	15.9	14.7	Gehman et al. 2018
<i>Daphnia dentifera</i> - <i>Metschnikowia bicuspidata</i>	Uninfected intrinsic growth rate	Spore load	$R_0$	26.0*	20.0*	26.0	Shocket et al. 2018b
<i>Daphnia magna</i> – <i>Ordospora colligata</i>	Lifetime reproduction	Spore load	$R_0$	16.2*	11.8*	18.8	Kirk et al. 2018, 2020

251 \*  $T_{opt}$  for these values was determined as the temperature at which the measure was maximized  
 252 along a range of discrete experimental temperatures, rather than the temperature maximizing the  
 253 measure along a fitted continuous curve, as is the case for each other value in the table. For  
 254 discrete temperature range used, see Supporting Information.

255 † The first number listed is individual-level host  $T_{opt}$ . The number in parentheses is population-  
 256 level  $T_{opt}$ .

257

258

259 **RESULTS**

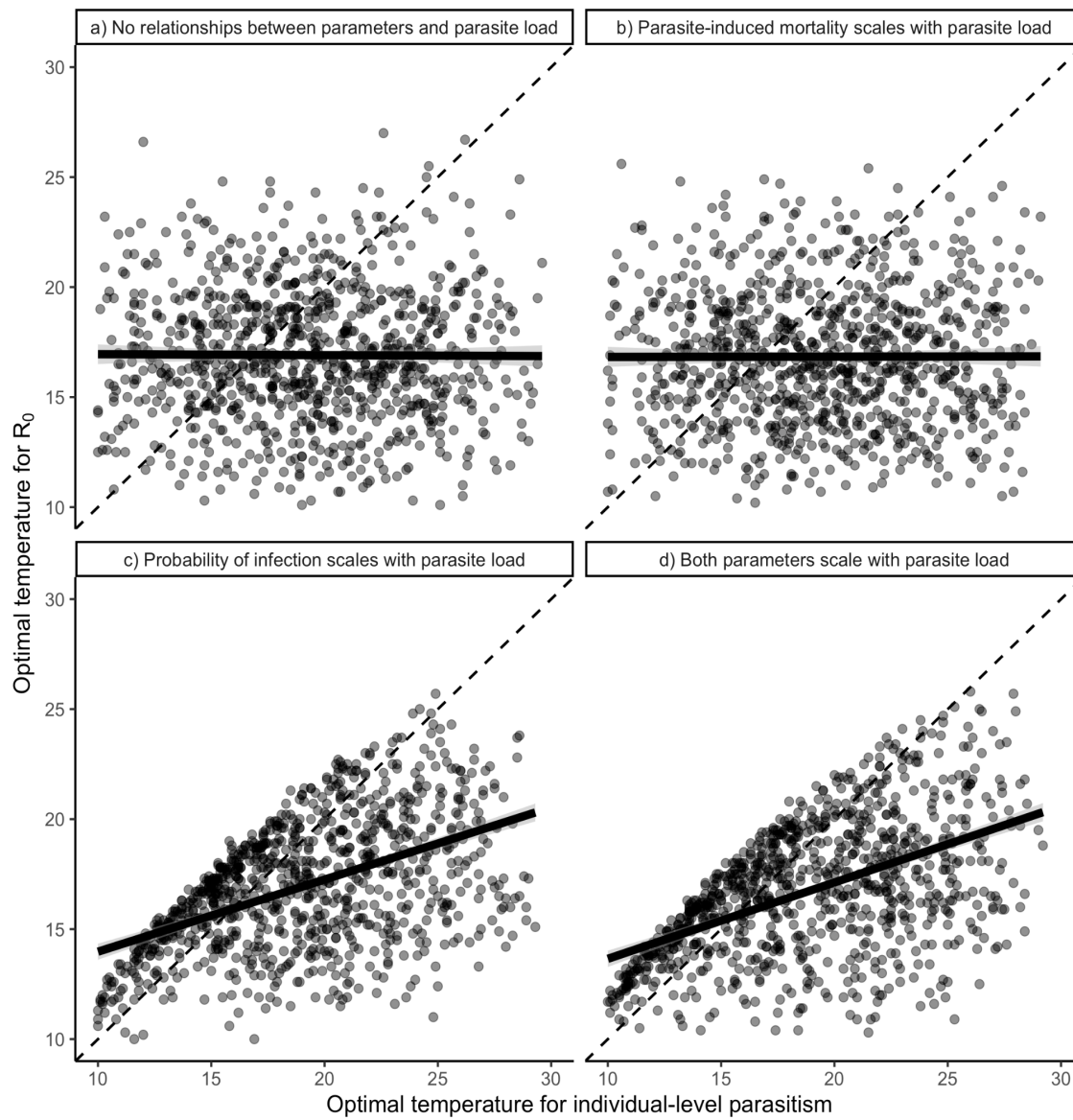
260 *Differences in host–parasite biology and the expected relationship between parasitism  $T_{opt}$*   
261 *across levels*

262 As hypothesized, the model showed that  $T_{opt}$  for individual- and population-level  
263 parasitism may be correlated or uncorrelated, depending on the relationships among the trait  
264 thermal responses. When the thermal responses of all parameters in the population-level  
265 parasitism model were independent from each other and from the thermal response of individual-  
266 level parasitism, we did not observe any relationship between the thermal optima of parasitism  
267 across levels (Fig. 1a). Similarly, there was no relationship between thermal optima in the  
268 scenario in which the thermal response of parasite-induced mortality was proportional to the  
269 thermal response of parasite load (Fig. 1b). This means that in this scenario, even though a  
270 parameter that partially determined the thermal response of population-level parasitism was  
271 directly dependent on the thermal response of individual-level parasitism, we still did not  
272 observe a relationship between the thermal optima. Conversely, when the probability of infection  
273 after contact was proportional to parasite load across the thermal range, we observed a strong,  
274 positive relationship between the thermal optima for parasitism across levels (Fig. 1c). Though  
275 the relationship was significant and positive, it does not fall upon the 1:1 line (95% confidence  
276 interval; Fig. 1c). Additionally, while many simulated host–parasite systems are observed below  
277 the 1:1 line (i.e., individual-level parasitism  $T_{opt}$  was greater than population-level parasitism  
278  $T_{opt}$ ), there were no systems in which population-level parasitism  $T_{opt}$  greatly exceeded  
279 individual-level parasitism  $T_{opt}$  under these model conditions. Finally, when both probability of  
280 infection after contact and parasite-induced mortality were proportional to parasite load across  
281 the thermal range, the correlation between individual-level parasitism  $T_{opt}$  and population-level

282 parasitism  $T_{opt}$  was strongly positive (Fig. 1d), closely resembling the scenario in which only  
283 probability of infection after contact was proportional to parasite load (Fig. 1c).

284

285



286

287 **Figure 1. Thermal optima of individual parasite burden may be either uncorrelated (top**  
288 **panels) or positively correlated (bottom panels) with thermal optima of  $R_0$  at the**  
289 **population level. The thermal optima of parasitism in 1000 simulated host–parasite systems at**  
290 **both the population level ( $R_0$ ) and individual level (parasite load) for four different modeled**  
291 **scenarios: a) no relationship between any parameters in the  $R_0$  model (Eq. 2) and parasite load**  
292 **(Eq. 1); b) parasite-induced mortality in the  $R_0$  model is proportional to parasite load; c)**  
293 **probability of infection after contact in the  $R_0$  model is proportional to parasite load; d) both**  
294 **parasite-induced mortality and probability of infection after contact in the  $R_0$  model are**  
295 **proportional to parasite load. Dashed black lines represent the 1:1 lines. Solid black lines and**  
296 **shaded bands represent the best fit linear regressions and 95% confidence intervals, respectively.**  
297

298 We found qualitatively similar results for several of our additional model scenarios.  
299 Specifically, we found similar results when thermal response parameters were drawn from  
300 normal distributions (Fig. S2), when parameter thermal breadth was larger (Fig. S3), when peak  
301 contact rates occurred at warmer temperatures (Fig. S4), and when the population-level  
302 parasitism model (Eq. 1) was altered to allow for chronic infections (Fig. S7) or for  
303 environmentally-transmitted parasites (Fig. S8). However, we found that adding a baseline level  
304 of individual-level parasitism across the temperature range, such that individual-level parasitism  
305 (and probability of infection when it is modeled as proportional to individual-level parasitism) is  
306 low but not zero when  $T < T_{\min}$  and  $T > T_{\max}$ , led to qualitatively different results when  
307 probability of infection was proportional to individual-level parasitism. In this case, a number of  
308 systems exhibited population-level parasitism  $T_{\text{opt}}$  much warmer than individual-level parasitism  
309  $T_{\text{opt}}$  (Fig. S5c-d), a pattern we did not observe in Figs. 1c-d. Allowing for individual-level  
310 parasitism to have a baseline level and for peak contact rates to occur at warmer temperatures led  
311 to even more systems with population-level parasitism  $T_{\text{opt}} \gg$  individual-level parasitism  $T_{\text{opt}}$   
312 (Fig. S6c-d).

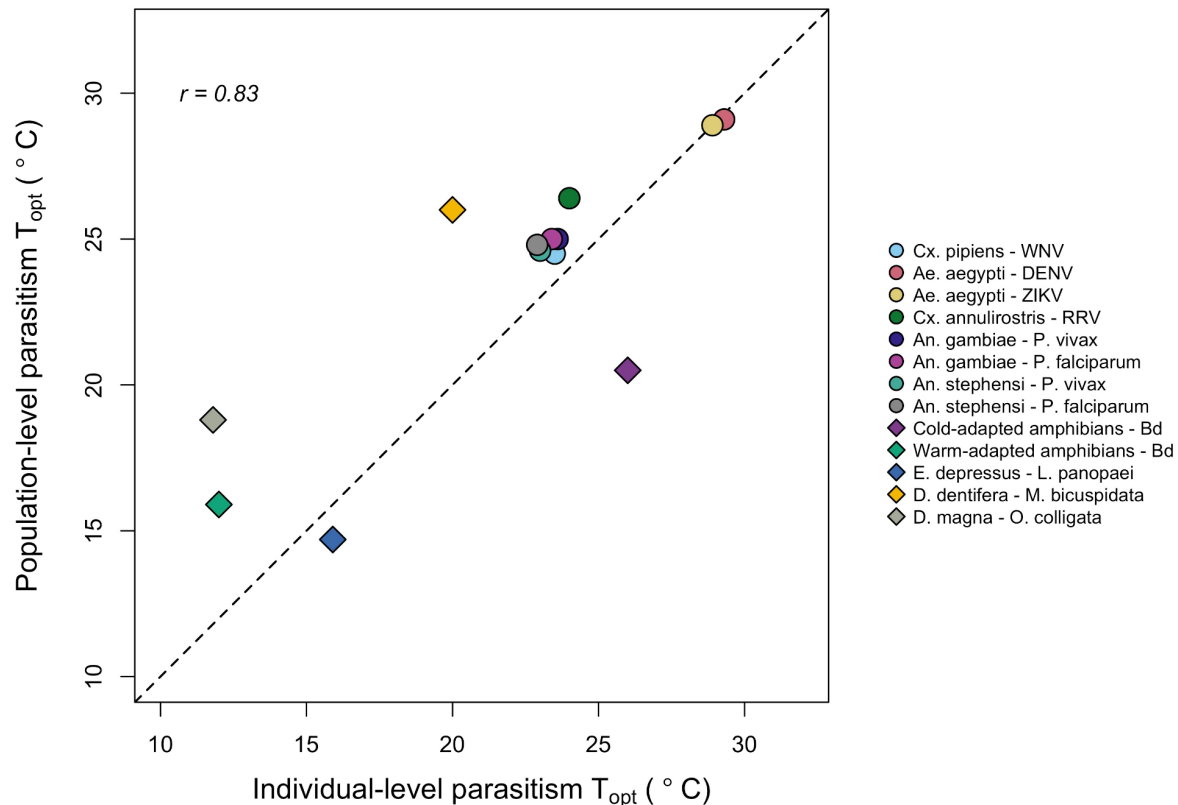
313

### 314 ***Relationship between parasitism $T_{\text{opt}}$ across levels in empirical systems***

315 The thirteen empirical systems we analyzed demonstrated a range of thermal optima for  
316 individual-level parasitism (11.8°C – 29.3°C) and population-level parasitism (14.7°C – 29.1°C).  
317 We found that population-level parasitism  $T_{\text{opt}}$  was significantly correlated with individual-level  
318 parasitism (Fig. 2; Pearson correlation = 0.83,  $p = 0.0005$ ,  $n = 13$ ). Of the thirteen systems, nine  
319 exhibited thermal optima at individual and population levels that were within 2.5°C of each  
320 other. The largest difference across levels appeared in the *D. magna*–*O. colligata* system in



321 which individual-level parasitism peaked at a temperature that is 7°C cooler than the peak for  
322 population-level parasitism. Nine of the thirteen systems exhibited higher thermal optima for  
323 population-level parasitism than individual-level parasitism, though in most cases this difference  
324 was small (Fig. 2; points above the dashed 1:1 line).



325  
326 **Figure 2. The thermal optima of population-level parasitism are positively correlated with**  
327 **the thermal optima of individual-level parasitism in empirical systems.** Points show  
328 estimates of the optimal temperature ( $T_{opt}$ ) for population-level parasitism versus  $T_{opt}$  of  
329 individual-level parasitism for thirteen host–parasite systems. We found a significant positive  
330 correlation between  $T_{opt}$  of population-level parasitism and  $T_{opt}$  of individual-level parasitism  
331 (Pearson correlation = 0.83,  $p = 0.0005$ ,  $n = 13$ ), and found that nine of the thirteen systems  
332 exhibited higher thermal optima for population-level parasitism than for individual-level  
333 parasitism (i.e., fall above the dashed 1:1 line). Circles represent mosquito – parasite systems and  
334 diamonds indicate non-mosquito – parasite systems.

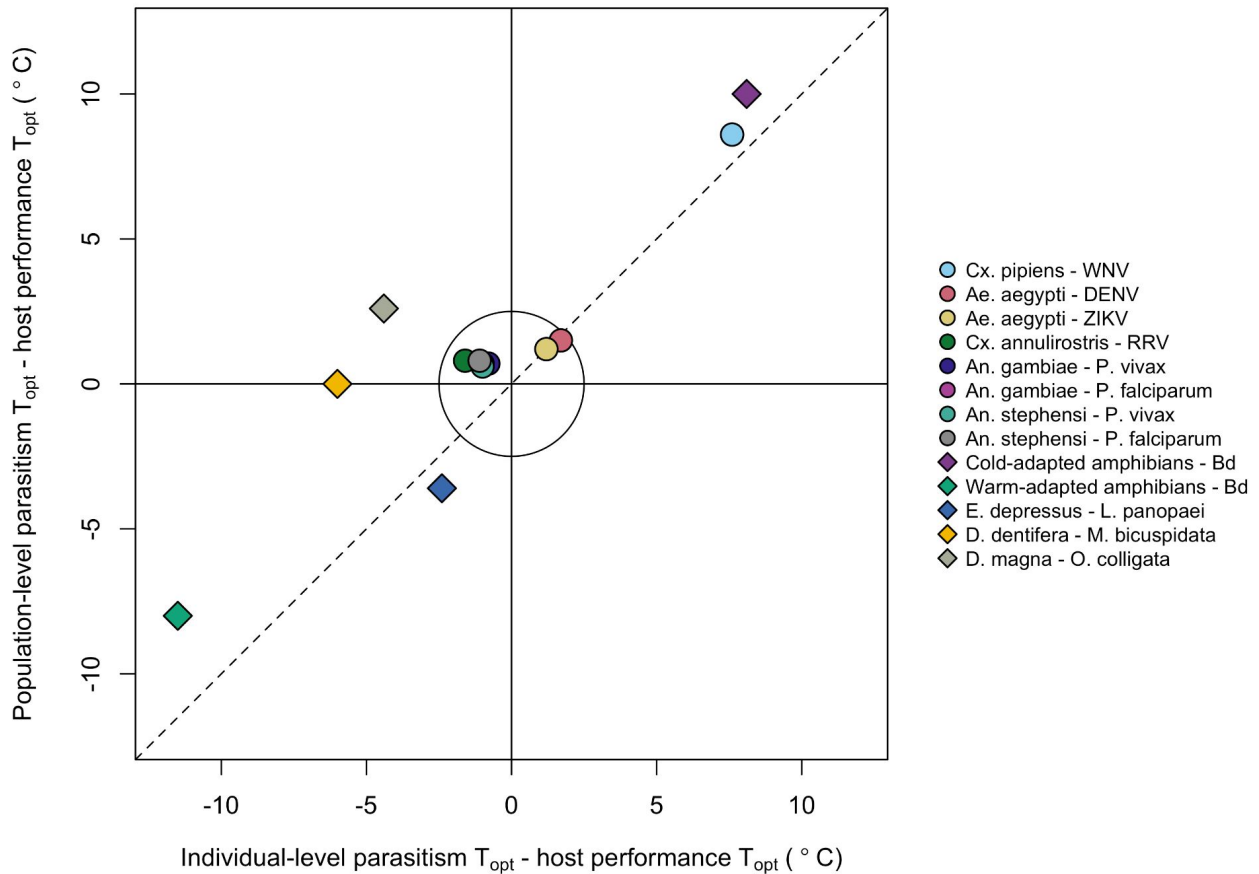
335

336

337 ***Relationship between parasitism  $T_{opt}$  and host performance  $T_{opt}$  in empirical systems***

338 Next, we compared the thermal optima of parasitism at both levels to  $T_{opt}$  for host  
339 performance (Fig. 3). If a system was situated at the origin in Fig. 3, it would have individual-  
340 level parasitism, population-level parasitism, and host performance maximized at the same  
341 temperature (i.e., no thermal mismatches exist). Displacement from the origin represents  
342 parasitism peaking at temperatures away from where host performance peaks (i.e., thermal  
343 mismatches at one or both levels). We found that over half (7/13) of the systems were situated  
344 close to the origin (arbitrarily defined here as within Euclidian distance of 2.5°C, represented by  
345 the circle in Fig. 3). However, all seven of these are mosquito–parasite systems, with the only  
346 mosquito system exhibiting strong thermal mismatches being *Cx. pipiens*–West Nile virus, in  
347 which both infected days and  $R_0$  peak at temperatures nearly 10°C higher than host performance  
348 (Fig. 3). The cold adapted amphibian–*B. dendrobatidis* system was also situated in the far upper-  
349 right quadrant (Fig. 3), showing strong thermal mismatches at both levels of parasitism, as  
350 shown in Cohen *et al.* (2017). Two systems showed cold-temperature mismatches at both levels:  
351 the crab *E. depressus*–*L. panopaei* and warm-adapted amphibian–*B. dendrobatidis* host–parasite  
352 systems. The zooplankton *D. dentifera*–*M. bicuspidata* system exhibited a thermal mismatch at  
353 cold temperatures at the individual level but no mismatch at the population level. Finally, the  
354 zooplankton *D. magna*–*O. colligata* system showed a distinct pattern of differing thermal  
355 mismatches across levels (Fig. 3): individual-level parasitism was maximized at a lower  
356 temperature than host performance while  $R_0$  peaked at a higher temperature than host  
357 performance. None of the thirteen systems showed positive individual-level mismatches but  
358 negative population-level mismatches; therefore, the lower-right quadrant of Fig. 3 is empty. The  
359 six systems that experienced thermal mismatches generally supported our hypothesis that if

360 mismatches occurred they would be at both levels and in the same direction, as more of these  
361 systems were situated in the upper-right or lower-left quadrants of Fig. 3 compared to the upper-  
362 left or lower-right quadrants.  
363



364  
365 **Figure 3. Thermal matches and mismatches tended to be correlated across levels of**  
366 **biological organization.** The difference between  $T_{opt}$  of population-level parasitism and host  
367 performance (y-axis) is plotted against the difference between  $T_{opt}$  of individual-level parasitism  
368 and host performance (x-axis) for thirteen host–parasite systems. Systems situated at the origin  
369 had population-level parasitism, individual-level parasitism, and host performance all maximized  
370 at the same temperature (i.e., no thermal mismatches exist), while displacement from the origin  
371 represents parasitism peaking at temperatures away from where host performance peaks (i.e.,  
372 thermal mismatches at individual or population levels). All seven of the systems situated close to  
373 the origin (within Euclidian distance of  $2.5^{\circ}\text{C}$ , represented by the black circle) were mosquito –  
374 parasite systems (circles; in contrast to systems with non-mosquito hosts: diamonds).  
375

376

## DISCUSSION

377

378

379

380

381

382

383

384

385

386

387

388

389

390

391

392

393

394

395

396

397

398

399

If we are to best predict how warming temperatures will affect host–parasite systems, we need to understand if effects on parasitism at one level of organization correspond with similar effects at another level. Moreover, understanding how these effects on parasitism compare to thermal effects on uninfected hosts can offer a more complete lens into how climate change will affect hosts. Our model found that small differences in the underlying biology of host–parasite systems can substantially alter the expected relationship between the thermal optima of parasitism in individual hosts and host populations, ranging from strong positive correlations to no correlation of  $T_{\text{opt}}$  across levels (Fig. 1). In our examination of thirteen empirical systems, we found a significant positive relationship between  $T_{\text{opt}}$  for parasitism at the two levels (Fig. 2). Additionally, while individual- and population-level parasitism both peaked at temperatures away from the host optimum in some systems, supporting the thermal mismatch hypothesis, this was not the case in seven of the eight mosquito–parasite systems (Fig. 3), suggesting thermal mismatches may be more common in certain types of host–parasite systems. Generally, our results show that information on the temperature-dependence, and specifically the thermal optimum, of a host–parasite system at either the individual- or population-level should provide a useful—though not quantitatively exact—baseline for predicting temperature dependence at the other level in a variety of host–parasite systems.

We found a significant positive correlation between  $T_{\text{opt}}$  of population-level parasitism and  $T_{\text{opt}}$  of individual-level parasitism, suggesting that the effects of warming on parasitism may often be in the same direction across levels. However, we also found that population-level parasitism tended to peak at slightly warmer temperatures than individual-level parasitism in the majority of systems (Fig. 2), meaning that these systems may experience small temperature ranges in which warming leads to increases in population-level parasitism but decreases in

400 individual-level parasitism. The greatest differences in  $T_{\text{opt}}$  were observed in the zooplankton *D.*  
401 *magna*–*O. colligata* system, the cold-adapted amphibians–*B. dendrobatidis* system, and the  
402 zooplankton *D. dentifera*–*M. bicuspidata* system (Fig. 2, Table 1). It is difficult to definitively  
403 parse out the causes of  $T_{\text{opt}}$  differences in the two amphibian systems since individual-level *Bd*  
404 parasitism was measured on either one or two frog species in the lab while population-level  
405 prevalence by the same parasite was synthesized across many field studies encompassing 235  
406 host species (Cohen *et al.* 2017). However, the *D. magna*–*O. colligata* system can provide an  
407 illuminating example. Contact rate in this host–microsporidian parasite system is maximized at  
408 30.1°C (Kirk *et al.* 2019). This is nearly 20°C warmer than  $T_{\text{opt}}$  for individual-level parasitism  
409 (11.8°C) and is thus one of the key factors that pulls the thermal optimum of  $R_0$  away from  
410 individual-level parasitism  $T_{\text{opt}}$  to a warmer temperature (18.8°C). Moreover, in the mosquito–  
411 parasite systems, which tended to have high population-level parasitism  $T_{\text{opt}}$  (Fig. 2), biting  
412 rate—a driver of host contact—usually has one of the highest optimal temperatures of all  
413 measured traits (Mordecai *et al.* 2013, 2017, 2019; Shocket *et al.* 2018a; Villena *et al.* 2020).  
414 These few systems represent only a small slice of the diversity of host–parasite systems that  
415 exist; however, they may represent a relatively greater portion of the diversity in thermal trait  
416 biology and temperature-dependent metabolic rates because these rates are often conserved  
417 across systems (Brown *et al.* 2004; Dell *et al.* 2011; Molnár *et al.* 2017). More empirical work  
418 measuring thermal responses of traits related to parasite transmission in other types of host–  
419 parasite systems, such as those with helminth or bacterial parasites—both of which have been  
420 shown to be affected by climate (Ben-Haim *et al.* 2003; Ben-Horin *et al.* 2013; Mignatti *et al.*  
421 2016)—can help broaden our perspective on the scaling of parasitism from individuals to  
422 populations in light of climate change.

423           The positive relationship observed for  $T_{\text{opt}}$  across levels in the thirteen empirical systems  
424 qualitatively matched the positive relationship observed in the two modeled scenarios in which  
425 probability of infection was proportional to parasite load (Fig. 1c-d). However, this should not be  
426 taken as evidence that these empirical systems follow the same described dynamics or meet the  
427 same assumptions of these modeled scenarios, as the underlying biology differs greatly between  
428 many of these systems, and the models that have been used to describe their dynamics differ both  
429 between the systems and from the simple model developed here (e.g., Briggs *et al.* 2010;  
430 Mordecai *et al.* 2017; Gehman *et al.* 2018; Shocket *et al.* 2018b; Kirk *et al.* 2020). Taken  
431 together, this means that the model results (Figs. 1, S2-S8) are useful for our understanding of  
432 how different  $T_{\text{opt}}$  relationships are possible under different plausible scenarios, but should not be  
433 used as statistical null hypotheses for our thirteen empirical systems. The contribution of this  
434 approach—pairing mechanistic models and thermal responses across biological levels under  
435 different assumptions—is that we can observe how different systems or thermal biology can lead  
436 to different patterns in  $T_{\text{opt}}$  across levels. Indeed, while our additional model scenarios generally  
437 supported our main finding that individual- and population-level parasitism can be correlated or  
438 uncorrelated and showed that this is qualitatively robust across different model structures and  
439 assumptions regarding thermal response shape, they also illustrated how changes to thermal  
440 biology can alter these patterns. For example, if peak contact rates tend to occur at warmer  
441 temperatures than other traits, we may observe more systems that have population-level  
442 parasitism  $T_{\text{opt}} >$  individual-level parasitism  $T_{\text{opt}}$  (Fig. S4). Also, despite not observing systems  
443 in the far upper-left space (where population-level parasitism  $T_{\text{opt}} \gg$  individual-level parasitism  
444  $T_{\text{opt}}$ ) for our model simulations when probability of infection scaled with individual-level

445 parasitism (Fig. 1c-d), additional scenarios showed that this is possible if individual-level  
446 parasitism does not decrease completely to zero when  $T < T_{\min}$  and  $T > T_{\max}$  (Figs. S5-S6).

447         The thermal mismatch hypothesis (Cohen *et al.* 2017, 2019a, b, 2020) has been proposed  
448 as an approach for understanding the effects of climate change on host–parasite systems,  
449 predicting that  $T_{\text{opt}}$  for parasitism should occur at temperatures away from host  $T_{\text{opt}}$  (i.e., a  
450 thermal mismatch) due to larger organisms (hosts) generally having narrower thermal breadth  
451 than smaller organisms (parasites; Rohr *et al.* 2018). While empirical evidence shows that  
452 thermal mismatches do occur at the population level across many systems (Cohen *et al.* 2020),  
453 the novel hypothesis we tested here is that thermal mismatches at the individual level will  
454 correspond with similar thermal mismatches at the population level. Of the five non-mosquito  
455 systems we explored—including the two amphibian–*Bd* systems investigated previously—  
456 parasitism tended to peak at temperatures away from the host’s optimum in each, meaning that  
457 these systems experience thermal mismatches at one or both levels. If our hypothesis was to be  
458 supported, we would expect most systems experiencing thermal mismatches to fall in the upper-  
459 right or lower-left quadrants of Fig. 3, rather than the upper-left or lower-right. We found that  
460 this was generally the case, with two systems experiencing thermal mismatches at warmer  
461 temperatures at both levels (Fig. 3; upper-right) and two systems experiencing thermal  
462 mismatches at cooler temperatures at both levels (Fig. 3; lower-left). The major exception was  
463 the *D. magna*–*O. colligata* system, in which host  $T_{\text{opt}}$  occurs at a temperature intermediate to the  
464 relatively cool  $T_{\text{opt}}$  for individual-level parasitism and relatively warm  $T_{\text{opt}}$  population-level  
465 parasitism (Fig. 3; upper-left). The other zooplankton host system we explored, *D. dentifera*–*M.*  
466 *bicuspidata*, exhibited a thermal mismatch at cooler temperatures at the individual level but no  
467 mismatch at the population level.

468 Evidence for thermal mismatches occurring at either level was weak in the mosquito–  
469 parasite systems. Seven of eight mosquito–parasite systems were situated close to the origin (Fig.  
470 3), suggesting that parasitism and host performance are maximized at close to the same  
471 temperatures and that no thermal mismatches are occurring at either level. Notably, when testing  
472 for thermal mismatches at the population level, (Cohen *et al.* 2020) also found that thermal  
473 mismatch effects were strongest in systems without vectors (or intermediate hosts). The  
474 exception in our study, *Cx. pipiens*–West Nile virus, in which parasitism at both levels peaks at  
475 temperatures much higher than host performance because *Cx. pipiens* adult lifespan is much  
476 longer at low temperatures (Shocket *et al.* 2020), is a system with a predominantly temperate  
477 distribution in North America, compared to the more sub-tropical and tropical distributions of  
478 malaria, dengue, Zika, Ross River virus, and their respective mosquito vectors. Why we  
479 observed this pattern in mosquito systems will require further investigation in different vector-  
480 borne systems across biological levels, including those systems with non-mosquito vectors such  
481 as ticks or sandflies.

482 We propose that situating host–parasite systems along both individual- and population-  
483 level axes as in Fig. 3 can provide a diagnostic framework for looking for thermal mismatches  
484 across biological levels. While our results do not conclusively address how general thermal  
485 mismatches at both levels may be, our finding that individual- and population-level  $T_{opt}$  are  
486 strongly related (Fig. 2) provides a general rule of thumb that, if a host–parasite system does  
487 experience thermal mismatches, they are likely to occur at both levels and in the same direction  
488 (though note the exception of *D. magna*–*O. colligata*; Fig. 3). This has major implications for  
489 our understanding of the effects of climate change on host-parasite systems, because if  $T_{opt}$  for  
490 both individual- and population-level parasitism is at a higher temperature than  $T_{opt}$  for host



491 performance, warming may not only decrease host performance itself, but also lead hosts to  
492 experience increasing effects of parasitism (Fig. 3; upper-right quadrant). Alternatively, if  $T_{opt}$   
493 for parasitism is at temperatures cooler than host performance optima, decreased host  
494 performance at warmer temperatures may be partially offset by decreased effects of parasitism  
495 (Fig. 3; lower-left quadrant). This is in line with recent projections that climate change may lead  
496 to hosts from cooler climates to experience increased parasitism, and hosts from warmer climates  
497 to experience decreased parasitism (Cohen *et al.* 2020).

498         To better understand how temperature affects parasitism and to make better predictions  
499 for how climate change will affect host–parasite systems across biological levels, we highlight  
500 two important research directions. First, when possible, studies that use experiments to  
501 investigate effects of temperature at the individual level can also be used to parameterize simple  
502 models of population-level parasitism (a ‘bottom-up’ approach). Second, field studies  
503 investigating population-level parasitism under different climate or weather conditions, often  
504 undertaken by measuring the proportion of individuals infected, should also aim to record  
505 measures of individual-level parasitism (a ‘top-down’ approach). The best direct measure would  
506 be to record the parasite load or an analogous metric measuring the parasite on or within the host,  
507 but in cases where this is not possible, indirect measures such as host condition may still be  
508 informative.

509         Overall, after our model illustrated that either positive or flat relationships between  $T_{opt}$   
510 across levels were plausible, we found a strong positive relationship in the thirteen systems we  
511 analyzed, suggesting that the effects of warming on individual-level outcomes may beget similar  
512 outcomes at the population level in various host–parasite systems. Many studies have  
513 investigated the effects of temperature on parasitism (reviewed, for example, in Marcogliese

514 2008; Lafferty 2009; Rohr *et al.* 2011; Altizer *et al.* 2013; Lafferty & Mordecai 2016; Claar &  
515 Wood 2020), though often at only one of either the individual or population levels. Our findings  
516 build upon these studies by emphasizing that how temperature affects individual-level parasitism  
517 can scale up to affect parasite transmission, prevalence, and the potential for epidemics in host  
518 populations, though not always in a 1:1 manner. While this is an important first step toward  
519 predicting the effects of climate change on systems by allowing researchers to primarily focus on  
520 parasitism at one level when necessary, future empirical work that investigates the thermal  
521 dependence of a wider range of host–parasite systems across levels, including in systems with  
522 different types of hosts (e.g., plants, non-amphibian vertebrates) and other types of parasites  
523 (e.g., helminths, bacterial parasites), will be necessary for investigating the generality of this  
524 result. More broadly, tying together more theory and empirical results to provide general  
525 predictions for how climate change will affect parasitism from individuals to ecosystems in a  
526 diverse range of hosts and parasites remains an urgent priority as accelerating climate change  
527 makes potentially catastrophic temperature increases of  $> 2^{\circ}\text{C}$  increasingly likely by 2050.  
528

## LITERATURE CITED

- 529  
530  
531 Altizer, S., Ostfeld, R.S., Johnson, P.T.J., Kutz, S. & Harvell, C.D. (2013). Climate Change and  
532 Infectious Diseases: From Evidence to a Predictive Framework. *Science*, 341, 514–519.  
533 Anderson, R.M. & May, R.M. (1978). Regulation and Stability of Host-Parasite Population  
534 Interactions: I. Regulatory Processes. *The Journal of Animal Ecology*, 47, 219.  
535 Anderson, R.M. & May, R.M. (1979). Population biology of infectious diseases: part 1. *Nature*,  
536 280, 361–367.  
537 Angilletta, M.J. (2006). Estimating and comparing thermal performance curves. *Journal of*  
538 *Thermal Biology*, 31, 541–545.  
539 Angilletta, M.J. (2009). *Thermal adaptation: a theoretical and empirical synthesis*. Oxford  
540 University Press.  
541 Ben-Ami, F., Regoes, R.R. & Ebert, D. (2008). A quantitative test of the relationship between  
542 parasite dose and infection probability across different host–parasite combinations. *Proc.*  
543 *R. Soc. B*, 275, 853–859.  
544 Ben-Haim, Y., Zicherman-Keren, M. & Rosenberg, E. (2003). Temperature-regulated bleaching  
545 and lysis of the coral *Pocillopora damicornis* by the novel pathogen *Vibrio coralliilyticus*.  
546 *AEM*, 69, 4236–4242.  
547 Ben-Horin, T., Lenihan, H.S. & Lafferty, K.D. (2013). Variable intertidal temperature explains  
548 why disease endangers black abalone. *Ecology*, 94, 161–168.  
549 Briere, J.-F., Pracros, P., Le Roux, A.-Y. & Pierre, J.-S. (1999). A Novel Rate Model of  
550 Temperature-Dependent Development for Arthropods. *Environ Entomol*, 28, 22–29.  
551 Briggs, C.J., Knapp, R.A. & Vredenburg, V.T. (2010). Enzootic and epizootic dynamics of the  
552 chytrid fungal pathogen of amphibians. *Proceedings of the National Academy of*  
553 *Sciences*, 107, 9695–9700.  
554 Brown, J.H., Gillooly, J.F., Allen, A.P., Savage, V.M. & West, G.B. (2004). TOWARD A  
555 METABOLIC THEORY OF ECOLOGY. *Ecology*, 85, 1771–1789.  
556 Bruno, J.F., Selig, E.R., Casey, K.S., Page, C.A., Willis, B.L., Harvell, C.D., *et al.* (2007).  
557 Thermal Stress and Coral Cover as Drivers of Coral Disease Outbreaks. *PLoS Biol*, 5,  
558 e124.  
559 Casey, T.M. (1976). Activity Patterns, Body Temperature and Thermal Ecology in Two Desert  
560 Caterpillars (Lepidoptera: Sphingidae). *Ecology*, 57, 485–497.  
561 Claar, D.C. & Wood, C.L. (2020). Pulse Heat Stress and Parasitism in a Warming World. *Trends*  
562 *in Ecology & Evolution*, 35, 704–715.  
563 Cohen, J.M., Civitello, D.J., Venesky, M.D., McMahon, T.A. & Rohr, J.R. (2019a). An interaction  
564 between climate change and infectious disease drove widespread amphibian declines.  
565 *Glob Change Biol*, 25, 927–937.  
566 Cohen, J.M., McMahon, T.A., Ramsay, C., Roznik, E.A., Sauer, E.L., Bessler, S., *et al.* (2019b).  
567 Impacts of thermal mismatches on chytrid fungus *Batrachochytrium dendrobatidis*  
568 prevalence are moderated by life stage, body size, elevation and latitude. *Ecol Lett*, 22,  
569 817–825.  
570 Cohen, J.M., Sauer, E.L., Santiago, O., Spencer, S. & Rohr, J.R. (2020). Divergent impacts of  
571 warming weather on wildlife disease risk across climates. *Science*, 370, eabb1702.  
572 Cohen, J.M., Venesky, M.D., Sauer, E.L., Civitello, D.J., McMahon, T.A., Roznik, E.A., *et al.*  
573 (2017). The thermal mismatch hypothesis explains host susceptibility to an emerging  
574 infectious disease. *Ecol Lett*, 20, 184–193.  
575 Day, T. (2001). Parasite transmission modes and the evolution of virulence. *Evolution*, 55,  
576 2389–2400.  
577 Dell, A.I., Pawar, S. & Savage, V.M. (2011). Systematic variation in the temperature  
578 dependence of physiological and ecological traits. *Proceedings of the National Academy*

- 579 *of Sciences*, 108, 10591–10596.
- 580 Ewald, P.W. (1983). Host-Parasite Relations, Vectors, and the Evolution of Disease Severity.
- 581 *Annu. Rev. Ecol. Syst.*, 14, 465–485.
- 582 Fenton, A. (2008). Worms and germs: the population dynamic consequences of microparasite-
- 583 macroparasite co-infection. *Parasitology*, 135, 1545–1560.
- 584 Fenton, A. (2013). Dances with worms: the ecological and evolutionary impacts of deworming
- 585 on coinfecting pathogens. *Parasitology*, 140, 1119–1132.
- 586 Frank, S.A. (1996). Models of Parasite Virulence. *The Quarterly Review of Biology*, 71, 37–78.
- 587 Gehman, A.-L.M., Hall, R.J. & Byers, J.E. (2018). Host and parasite thermal ecology jointly
- 588 determine the effect of climate warming on epidemic dynamics. *Proc Natl Acad Sci USA*,
- 589 115, 744–749.
- 590 Handel, A. & Rohani, P. (2015). Crossing the scale from within-host infection dynamics to
- 591 between-host transmission fitness: a discussion of current assumptions and knowledge.
- 592 *Phil. Trans. R. Soc. B*, 370, 20140302.
- 593 Harvell, C.D., Montecino-Latorre, D., Caldwell, J.M., Burt, J.M., Bosley, K., Keller, A., *et al.*
- 594 (2019). Disease epidemic and a marine heat wave are associated with the continental-
- 595 scale collapse of a pivotal predator (*Pycnopodia helianthoides*). *Sci. Adv.*, 5, eaau7042.
- 596 van der Have, T.M. (2002). A proximate model for thermal tolerance in ectotherms. *Oikos*, 98,
- 597 141–155.
- 598 Huey, R.B. & Kingsolver, J.G. (1989). Evolution of thermal sensitivity of ectotherm performance.
- 599 *Trends in Ecology & Evolution*, 4, 131–135.
- 600 Huey, R.B. & Stevenson, R.D. (1979). Integrating Thermal Physiology and Ecology of
- 601 Ectotherms: A Discussion of Approaches. *American Zoologist*, 19, 357–366.
- 602 Kirk, D., Jones, N., Peacock, S., Phillips, J., Molnár, P.K., Krkošek, M., *et al.* (2018). Empirical
- 603 evidence that metabolic theory describes the temperature dependency of within-host
- 604 parasite dynamics. *PLoS Biol*, 16, e2004608.
- 605 Kirk, D., Luijckx, P., Jones, N., Krichel, L., Pencer, C., Molnár, P., *et al.* (2020). Experimental
- 606 evidence of warming-induced disease emergence and its prediction by a trait-based
- 607 mechanistic model. *Proc. R. Soc. B.*, 287, 20201526.
- 608 Kirk, D., Luijckx, P., Stanic, A. & Krkošek, M. (2019). Predicting the Thermal and Allometric
- 609 Dependencies of Disease Transmission via the Metabolic Theory of Ecology. *The*
- 610 *American Naturalist*, 193, 661–676.
- 611 Koelle, K., Pascual, M. & Yunus, M. (2005). Pathogen adaptation to seasonal forcing and
- 612 climate change. *Proc. R. Soc. B*, 272, 971–977.
- 613 Kordas, R.L., Harley, C.D.G. & O'Connor, M.I. (2011). Community ecology in a warming world:
- 614 The influence of temperature on interspecific interactions in marine systems. *Journal of*
- 615 *Experimental Marine Biology and Ecology*, 400, 218–226.
- 616 Lafferty, K.D. (2009). The ecology of climate change and infectious diseases. *Ecology*, 90, 888–
- 617 900.
- 618 Lafferty, K.D. & Mordecai, E.A. (2016). The rise and fall of infectious disease in a warmer world.
- 619 *F1000Res*, 5, 2040.
- 620 Marcogliese, D.J. (2008). The impact of climate change on the parasites and infectious
- 621 diseases of aquatic animals. *Rev. scij. tech. Off. init. Epiz.*, 27, 467–484.
- 622 McCallum, H., Fenton, A., Hudson, P.J., Lee, B., Levick, B., Norman, R., *et al.* (2017). Breaking
- 623 beta: deconstructing the parasite transmission function. *Phil. Trans. R. Soc. B*, 372,
- 624 20160084.
- 625 Mideo, N., Nelson, W.A., Reece, S.E., Bell, A.S., Read, A.F. & Day, T. (2011). Bridging scales
- 626 in the evolution of infectious disease life histories: application. *Evolution*, 65, 3298–3310.
- 627 Mignatti, A., Boag, B. & Cattadori, I.M. (2016). Host immunity shapes the impact of climate
- 628 changes on the dynamics of parasite infections. *Proc Natl Acad Sci USA*, 113, 2970–
- 629 2975.

- 630 Molnár, P.K., Sckrabulis, J.P., Altman, K.A. & Raffel, T.R. (2017). Thermal Performance Curves  
631 and the Metabolic Theory of Ecology—A Practical Guide to Models and Experiments for  
632 Parasitologists. *Journal of Parasitology*, 103, 423.
- 633 Mordecai, E.A., Caldwell, J.M., Grossman, M.K., Lippi, C.A., Johnson, L.R., Neira, M., *et al.*  
634 (2019). Thermal biology of mosquito-borne disease. *Ecol Lett*, 22, 1690–1708.
- 635 Mordecai, E.A., Cohen, J.M., Evans, M.V., Gudapati, P., Johnson, L.R., Lippi, C.A., *et al.*  
636 (2017). Detecting the impact of temperature on transmission of Zika, dengue, and  
637 chikungunya using mechanistic models. *PLoS Negl Trop Dis*, 11, e0005568.
- 638 Mordecai, E.A., Paaijmans, K.P., Johnson, L.R., Balzer, C., Ben-Horin, T., de Moor, E., *et al.*  
639 (2013). Optimal temperature for malaria transmission is dramatically lower than  
640 previously predicted. *Ecol Lett*, 16, 22–30.
- 641 Pedersen, A.B. & Antonovics, J. (2013). Anthelmintic treatment alters the parasite community in  
642 a wild mouse host. *Biol. Lett.*, 9, 20130205.
- 643 R Core Team. (2020). R: A language and environment for statistical computing. R Foundation  
644 for Statistical Computing, Vienna, Austria. URL <https://www.R-project.org/>.
- 645 Rohr, J.R., Civitello, D.J., Cohen, J.M., Roznik, E.A., Sinervo, B. & Dell, A.I. (2018). The  
646 complex drivers of thermal acclimation and breadth in ectotherms. *Ecol Lett*, 21, 1425–  
647 1439.
- 648 Rohr, J.R., Dobson, A.P., Johnson, P.T.J., Kilpatrick, A.M., Paull, S.H., Raffel, T.R., *et al.*  
649 (2011). Frontiers in climate change—disease research. *Trends in Ecology & Evolution*,  
650 26, 270–277.
- 651 Shocket, M.S., Ryan, S.J. & Mordecai, E.A. (2018a). Temperature explains broad patterns of  
652 Ross River virus transmission. *eLife*, 7, e37762.
- 653 Shocket, M.S., Strauss, A.T., Hite, J.L., Šljivar, M., Civitello, D.J., Duffy, M.A., *et al.* (2018b).  
654 Temperature Drives Epidemics in a Zooplankton-Fungus Disease System: A Trait-  
655 Driven Approach Points to Transmission via Host Foraging. *The American Naturalist*,  
656 191, 435–451.
- 657 Shocket, M.S., Verwillow, A.B., Numazu, M.G., Slamani, H., Cohen, J.M., El Moustaid, F., *et al.*  
658 (2020). Transmission of West Nile and five other temperate mosquito-borne viruses  
659 peaks at temperatures between 23°C and 26°C. *eLife*, 9, e58511.
- 660 Tesla, B., Demakovskiy, L.R., Mordecai, E.A., Ryan, S.J., Bonds, M.H., Ngonghala, C.N., *et al.*  
661 (2018). Temperature drives Zika virus transmission: evidence from empirical and  
662 mathematical models. *Proc. R. Soc. B*, 285, 20180795.
- 663 Thomas, M.B. & Blanford, S. (2003). Thermal biology in insect-parasite interactions. *Trends in*  
664 *Ecology & Evolution*, 18, 344–350.
- 665 Villena, O.C., Ryan, S.J., Murdock, C.C. & Johnson, L.R. (2020). Temperature impacts the  
666 transmission of malaria parasites by *Anopheles gambiae* and *Anopheles stephensi*  
667 mosquitoes. *bioRxiv*, <https://doi.org/10.1101/2020.07.08.194472>.